40-Gb/s Optical Clock Recovery Using a Compact Traveling-Wave Electroabsorption Modulator-Based Ring Oscillator

Zhaoyang Hu, Hsu-Feng Chou, John E. Bowers, *Fellow, IEEE*, and Daniel J. Blumenthal, *Fellow, IEEE*

***Abstract*—Compact optical clock recovery is demonstrated by utilizing filtered and amplified photocurrent in a traveling-wave electroabsorption modulator. The 40-GHz optical clock was recovered from a 40-Gb/s optical time-division multiplexed signal and transferred to a new clock wavelength. The recovered optical clock has 500-fs timing jitter and 8-ps pulsewidth.**

***Index Terms*—Clock recovery, electroabsorption modulator (EAM), optical data processing, regeneration.**

I. Introduction

RETIMING, reshaping, and amplification regeneration (3R) is considered a key-function for the future long-haul all-optical networks [1]. In 3R optical regenerative wavelength conversion, optical clock recovery (OCR) is performed first and the recovered clock pulses are launched into a regenerative wavelength converter along with the original data signal allowing it to be reshaped and retimed as it is converted to a new wavelength. To date, OCR based on an electrooptical phase-locked loop has been proposed and demonstrated [2], [3]. Although these approaches resulted in a high quality recovered clock, a more compact solution is preferred for practical use. Self-pulsating distributed feedback lasers have been applied for OCR and they have a compact structure [4], [5]. Injection-locked optoelectronic oscillator-based OCR was also demonstrated with high spectral purity but it requires a relatively more complicated configuration which involves conversion between optical and electrical signals with a photodetector and the feedback of the electrical signal to an electrooptical modulator [6], [7].

In this letter, we demonstrate a compact 40-Gb/s OCR using a traveling-wave electroabsorption modulator (TW-EAM)-based ring oscillator, shown as the shadowed box in Fig. 1. Details of the TW-EAM have been previously reported in [8]. The TW-EAM is ribbon-bonded to a chip coplanar Q filter, which detects and filters the clock component of the input optical signal. When the OCR's oscillation frequency is tuned close to the clock frequency, the ring oscillator is injection phase-locked. The TW-EAM simultaneously works as a photodetector by using photocurrent from the upper electrical port and a pulsed optical clock generator by applying the radio frequency (RF) feedback driving signal on the lower electrical port to modulate the continuous-wave (CW) light at another wavelength [9].

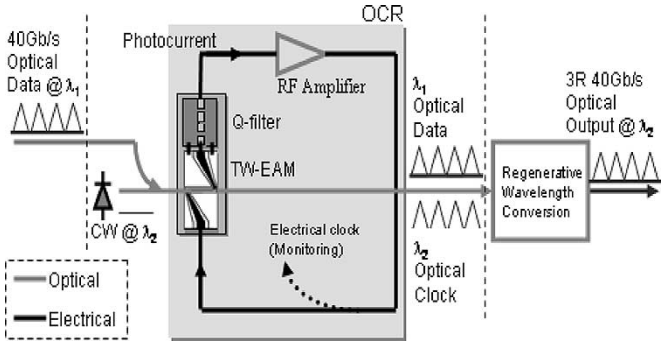

Fig. 1. 3R architecture using the proposed OCR.

The output signals of the OCR are the data signal (λ_1) and the recovered optical clock (λ_2). These signals can be launched into a subsequent regenerative wavelength converter to achieve 3R conversion to λ_2. In contrast to the injection locked optoelectronic oscillator, this approach is more compact and can be fully integrated on a chip. Also, due to the nonlinear electroabsorption process of the TW-EAM, a phase shifter is not employed in the ring oscillator because the loop phase can be tuned by adjusting the bias voltage. This effect is supported by the analytical model presented in the letter. On the other hand, the usual photodetector in the injection-locked optoelectronic oscillator cannot provide such phase shift due to the constant responsivity. Through tuning the reverse bias of the TW-EAM, the oscillation frequency was measured to shift up to $\pm$400 kHz under optical injection.

II. Analytical Model at Locking Condition

In a TW-EAM, the electroabsorption process generates an electric-field-dependent photocurrent $I_{\rm ph} = \eta_m(V)P_{\rm opt}$, where $P_{\rm opt}$ is the input optical power and $\eta_m(V)$ is the responsivity. Here, we consider a simple case under locking to simplify the analysis of the OCR's operation. When an optical signal $p_{\rm opt}(t) = p_0 + p\cos\omega_{\rm in}t$ enters the TW-EAM driven by a dc reverse bias V_b and an RF voltage signal $V_m\cos(\omega_{\rm in}t+\phi)$ (the oscillating signal in the loop), the generated photocurrent is given by

$$I_{\rm ph} = \eta_m\left[V_b + V_m\cos\left(\omega_{\rm in}t+\phi\right)\right] \bullet \left(p_0 + p\cos\omega_{\rm in}t\right) \quad (1)$$

Manuscript received December 5, 2003; revised January 9, 2004. This work was supported by KDDI under Grant 442530-59406, and by the State of California UCDiscovery Grant 597095-19929.

The authors are with the Department of Electrical and Computer Engineering, University of California, Santa Barbara, CA 93106-9560 USA (e-mail: huby@ece.ucsb.edu).

Digital Object Identifier 10.1109/LPT.2004.826056

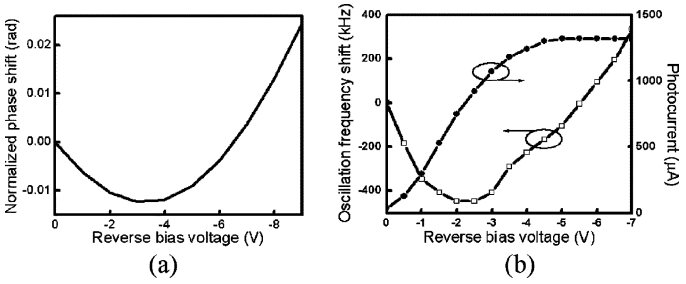

Fig. 2. (a) Simulation result of the relationship between the normalized phase shift and the reverse bias ($A = -64.11176$, $B_1 = -492.013\,61$, $B_2 = -42.664\,19$, $g = 9.9$, $\alpha = 0.1$). (b) Measured result of the oscillation frequency shift (square symbol curve) and TW-EAM photocurrent (circle symbol curve).

where ϕ is the phase of the RF signal relative to the optical signal, and $\eta_m(V)$ can be approximated as a second-order polynomial $A + B_1V + B_2V^2$ based on the measured relationship between photocurrent and reverse bias voltage, as shown in Fig. 2(b). The generated photocurrent along with the transmitted RF signal $\alpha V_m \cos(\omega_{\text{in}}t + \phi)$ are filtered at ω_{in} by the Q filter, amplified with net loop voltage gain g, and then fed back to the lower electrical port of the TW-EAM as

$$V'(t) = V_1 \cos\left[\omega_{\text{in}}(t+\tau) + \phi_1\right] \tag{2}$$

where α is the insertion loss of the TW-EAM, τ is the loop delay, V_1 is the voltage amplitude, and ϕ_1 is the extra phase change of the feedback signal. In order to achieve oscillation, every roundtrip signal must exactly replicate the initial signal. Therefore, the injection locked oscillation conditions for both amplitude (3a) and phase (3b) are

$$V_1 = V_m \tag{3a}$$

$$\phi_1 + \omega_{\text{in}}\tau = \phi + 2N\pi \tag{3b}$$

where N is an integer. Furthermore, ω_{in} can be written in the form of $\omega_{\text{in}} = \omega_{\text{osc}} + \Delta\omega$, where ω_{osc} is the eigenmode frequency of the ring oscillator and $\Delta\omega$ is the frequency shift due to the extra phase change ϕ_1. We numerically simulated the influence of the reverse bias on the loop phase shift (leading to $\Delta\omega$), as shown in Fig. 2(a), where p_0 and p were set as 10 and 0.5 mW in the calculation. We also measured the shift in oscillation frequency by using a 20-dB monitor-T to tap out the electrical signal, which is shown in Fig. 2(b). The oscillation frequency can be shifted up to $\pm$400 kHz by tuning the reverse bias voltage. Obviously, there is a tradeoff between selecting an optimal bias point for the pulse generation and wide tuning of the oscillation frequency. However, this problem can be minimized if only fine tuning is required by adjusting the bias when accurate loop length is obtained by monolithic integration.

III. Experimental Results

A 10-GHz gain-switched distributed Bragg reflector laser was used to generate pulses at 1553.8 nm (λ_1) and modulated with $2^{31} - 1$ pseudorandom binary sequence pattern by a $LiNbO_3$ modulator and then multiplexed to 40-Gb/s optical time-division multiplexing (OTDM) signal. The CW light input for generating the recovered optical clock was 6 dBm at

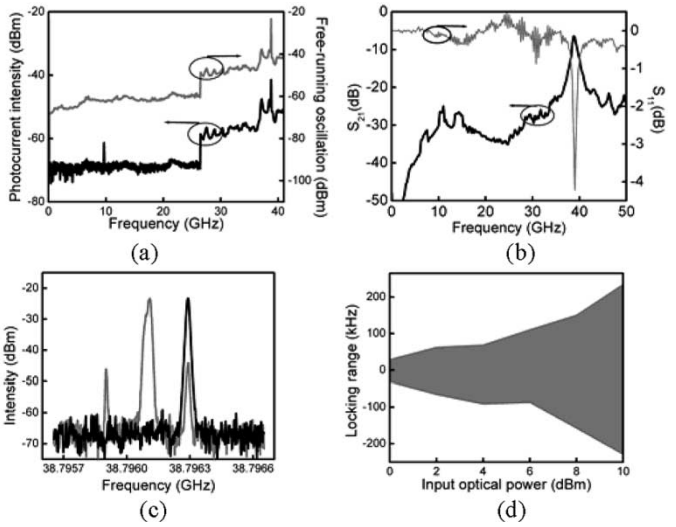

Fig. 3. (a) RF spectra of TW-EAM's photocurrent (lower dark curve) and the OCR free-running oscillation (upper gray curve). (b) S parameters of 40-GHz Q filter. (c) RF spectra of noninjection locked (gray line) and injection locked (dark line) optical output. (d) OCR's locking range.

1558.7 nm (λ_2). The TW-EAM used in the OCR has a total extinction ratio of above 30 dB for the transverse-magnetic mode. Its 3-dB bandwidth as a photodetector is 12 GHz but the rolloff is slow [9]. At 6-dBm input power of ~40-Gb/s OTDM signal, the RF spectrum of TW-EAM's photocurrent is shown as the lower curve in Fig. 3(a) and ~40-GHz tone is -40 dBm. The peak around 10 GHz comes from imperfect 1 : 4 multiplexing. The 40-GHz chip coplanar Q filter is realized by creating a capacitively coupled resonant section in the inner conductor [10]. It was fabricated on a semi-insulated InP substrate with a Q factor of about 50 and a sideband suppression ratio of over 20 dB, which is shown in Fig. 3(b). It was bonded to the TW-EAM using 50-μm-wide gold ribbons. A 38–40-GHz RF amplifier with 26-dB gain was used for compensating the loop loss and a bias-tee was used to provide the reverse bias for the TW-EAM.

Without optical signal input, the OCR oscillated at the frequency of 38.7961 GHz which is determined by the peak frequency of Q filter and the loop length, as shown by the upper curve in Fig. 3(a). When a ~40-Gb/s OTDM signal is applied, both the 38.796 29-GHz clock component and the free-running mode exist in the loop, shown as the gray line in Fig. 3(c). Through adjusting TW-EAM's reverse bias voltage to 3 V, the OCR oscillation frequency was tuned close to the input data frequency and its phase was also locked, shown as the dark line in Fig. 3(c). The RF power in the loop was estimated to be 12 dBm by using the monitor-T. The locking range was measured to be above 400 kHz at 10-dBm optical input power, as shown in Fig. 3(d).

The output optical signal was amplified and 2.4-nm optical bandpass filters were used to separate the ~40-GHz generated optical clock at 1558.7 nm and the OTDM signal at 1553.8 nm. Fig. 4(a) and (b) shows the ~40-Gb/s input OTDM signal and ~40-GHz recovered optical clock. The optical spectrum of the generated optical clock is shown in Fig. 4(c) and its pulsewidth is ~8 ps, as shown in the inset. The optical extinction ratio of recovered optical clock is estimated to be over 15 dB from its

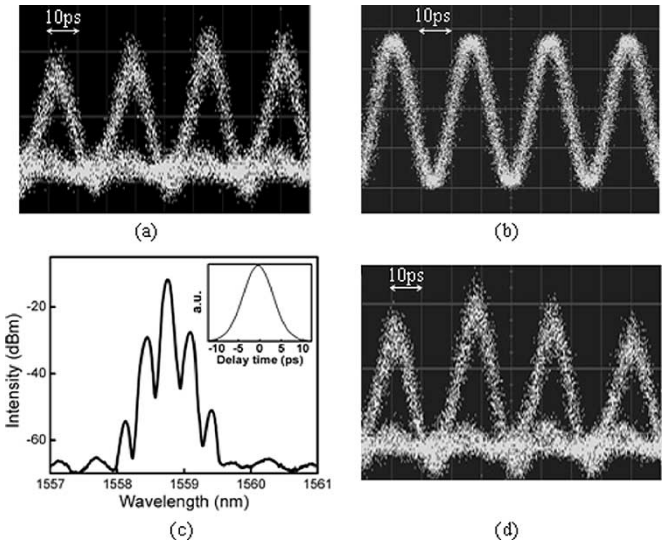

Fig. 4. (a) Eye diagram of ∼40-Gb/s input OTDM signal. (b) ∼40-GHz generated optical clock and (c) its optical spectrum (resolution bandwidth: 0.1 nm) and autocorrelation curve (inset). (d) Eye diagram of output OTDM signal.

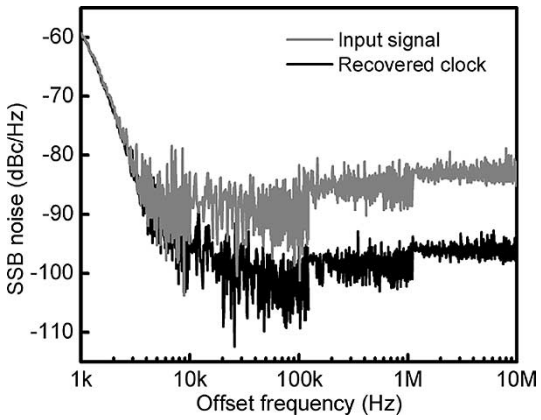

Fig. 5. SSB noise spectra of the input OTDM signal and optical recovered clock (resolution bandwidth: 1 kHz).

optical spectrum in Fig. 4(c). No data transfer due to cross absorption modulation was observed because of the relatively low optical input power. The TW-EAM introduced ∼20-dB insertion loss, however, the eye diagrams of output OTDM signal are clear after erbium-doped fiber amplifier (EDFA) amplification, shown as Fig. 4(d). No significant difference was observed when compared to the original input signal even though the modulation effect of the recovered electrical clock could suppress the interchannel crosstalk [11]. The OCR's capture time for synchronization to the data stream mainly depends on the loop length. In the experiment, the loop length is about 1 m, which implies microsecond-order capture time.

Fig. 5 depicts the single sideband (SSB) noise spectra of the input OTDM signal and the generated optical clock (with EDFA amplification). Through integrating the noise spectra from offset frequency of 1 kHz to 10 MHz, the root-mean-square (rms) timing jitters for the input OTDM signal and the recovered optical clock are 830 and 500 fs, respectively. The OCR locks to the line-rate frequency while suppressing other frequency components (harmonics and subharmonics) associated with the input signal, which reduces the timing jitter.

IV. Conclusion

We have demonstrated a compact 40-GHz OCR using a TW-EAM-based ring oscillator. An analytical model at locking condition for the OCR operation was also presented, which supports the phase tuning mechanism in the ring oscillator. The recovered 40-GHz optical clock has 500-fs rms timing jitter, 8-ps pulsewidth, and 400-kHz locking range. The timing jitter of recovered optical clock is lower than the input OTDM signal due to spectral purification effect of the OCR. The proposed compact structure consisting of a TW-EAM, a coplanar Q filter, and an RF amplifier is promising for fast OCR provided that monolithic integration is realized to minimize the loop length and hence the corresponding capture time for synchronization.

References

[1] T. Otani, T. Miyazaki, and S. Yamamoto, "40-Gb/s optical 3R regenerator using electroabsorption modulators for optical networks," *J. Lightwave Technol.*, vol. 20, pp. 195–200, Feb. 2002.

[2] D. T. K. Tong, K.-L. Deng, B. Mikkelsen, G. Raybon, K. F. Dreyer, and J. E. Johnson, "160 Gbit/s clock recovery using electroabsorption modulator-based phased-locked loop," *Electron. Lett.*, vol. 36, pp. 1951–1952, 2001.

[3] E. S. Awad, P. S. Cho, N. Moulton, and J. Goldhar, "All-optical timing extraction with simultaneous optical demultiplexing using time-dependant loss saturation in electroabsorption modulator," presented at the Conf. Lasers and Electro-Optics (CLEO 2002), Long Beach, CA, Paper CPDB9-1.

[4] C. Bornholdt, B. Sartorius, S. Schelhase, M. Möhrle, and S. Bauer, "Self-pulsating DFB-laser for all-optical clock recovery at 40 Gb/s," *Electron. Lett.*, vol. 36, pp. 327–328, 2000.

[5] W. Mao, Y. Li, M. Al-Mumin, and G. Li, "All-optical clock recovery from RZ-format data by using a two-section gain-coupled DFB laser," *J. Lightwave Technol.*, vol. 20, pp. 1705–1714, Sept. 2002.

[6] X. S. Yao and G. Lutes, "A high-speed photonic clock and carrier recovery device," *IEEE Photon. Technol. Lett.*, vol. 8, pp. 688–691, May 1996.

[7] L. Huo, Y. Dong, C. Lou, and Y. Gao, "Clock extraction using optoelectronic oscillator from high-speed NRZ signal and NRZ-to-RZ format transformation," *IEEE Photon. Technol. Lett.*, vol. 15, pp. 981–983, July 2003.

[8] Y.-J. Chiu, H.-F. Chou, V. Kaman, P. Abraham, and J. E. Bowers, "High extinction ratio and saturation power traveling-wave electroabsorption modulator," *IEEE Photon. Technol. Lett.*, vol. 14, pp. 792–794, June 2002.

[9] H.-F. Chou, Z. Hu, J. E. Bowers, D. J. Blumenthal, K. Nishimura, R. Inohara, and M. Usami, "Simultaneous 160-Gb/s demultiplexing and clock recovery by utilizing microwave harmonic frequencies in a traveling-wave electroabsorption modulator," *IEEE Photon. Technol. Lett.*, vol. 16, pp. 608–610, Feb. 2004.

[10] D. F. Williams and S. E. Schwarz, "Design and performance of coplanar waveguide bandpass filters," *IEEE Trans. Microwave Theory Tech.*, vol. MTT-83, pp. 558–566, July 1983.

[11] K. Nishmura, M. Tsurusawa, and M. Usami, "Novel all-optical 3R regenerator using cross-absorption modulation in RF-driven electroabsorption waveguide," in *Proc. 2001 Eur. Conf. Optical Communication*, pp. 286–287.